J Oral Pathol Med (2006) 35: 278–85

www.blackwellmunksgaard.com/jopm

Oligonucleotide microarray analysis of ameloblastoma compared with dentigerous cyst

Jijun Lim[1], Hyowon Ahn[2], Sunhong Min[2], Seong-Doo Hong[1], Jae-Il Lee[1], Sam-Pyo Hong[1]

[1]*Department of Oral Pathology, Dental School, Dental Research Institute, Seoul National University, Jongno-gu, Seoul;* [2]*Dental School, Seoul National University, Jongno-gu, Seoul, Korea*

BACKGROUND: Ameloblastoma is a benign, but locally invasive tumor known for its high rate of recurrence. However, few comprehensive genetic studies have been conducted about its tumorigenesis. Our aim was to identify possible genes involved in the development and progression of ameloblastoma, using microarray analysis with dentigerous cyst as a control.

METHODS: Total RNA was extracted from two fresh dentigerous cysts and ameloblastoma specimens. Following microarray analysis, semiquantitative reverse transcription–polymerase chain reaction (RT–PCR) and immunohistochemistry were performed on selected genes.

RESULTS: Seventy-three genes were overexpressed and 49 were underexpressed. These genes were divided into categories according to function. The microarray results for 13 selected genes were verified with semiquantitative RT–PCR.

CONCLUSIONS: We identified important genes related to the development and progression of ameloblastoma through a large-scale gene expression analysis. This study will stimulate further investigations on genes significant for early diagnosis and prognosis of ameloblastoma.

J Oral Pathol Med (2006) **35**: 278–85

Keywords: ameloblastoma; dentigerous cyst; microarray

Introduction

Ameloblastoma is a benign but locally invasive tumor known for its high rate of recurrence. As it is the most common odontogenic tumor (1), it is important to investigate its etiology. Many ameloblastomas have been known to develop from odontogenic cysts, such as dentigerous cyst. Dentigerous cyst is the second most common odontogenic cyst, accounting for approximately 20% of all true cysts in the jaw (2). Much has been written about the possibility that the lining of a dentigerous cyst might undergo neoplastic transformation to an ameloblastoma (3–5). We compared differences in gene expression between the dentigerous cyst and ameloblastoma using microarray analysis for the first time. There have only been two previous microarray studies on ameloblastoma, in which cDNA probes were used and gene expression compared with human tooth germs or other tumors (6, 7). Our study used oligonucleotide probes and the dentigerous cysts as a control in order to better identify possible genes that participate in its neoplastic transformation into an ameloblastoma.

Correspondence: Sam-Pyo Hong, Department of Oral Pathology, Dental School, Dental Research Institute, Seoul National University, 28-2 Yongon-dong, Jongno-gu, Seoul 110-744, Korea. Tel: 82-2-2072-2637. Fax: 82-2-766-4544. E-mail: hongsp@snu.ac.kr
Accepted for publication September 1, 2005

Materials and methods

Tissue preparation

Two fresh dentigerous cyst and two fresh ameloblastoma specimens (one male, one female, aged 17 and 34 years, plexiform and acanthomatous, both from mandibular molar area) were removed during surgery, at Seoul National University Dental Hospital in South Korea, frozen in liquid nitrogen, and stored at −70°C for microarray analysis. Fifty-four paraffin-embedded tissue sections (ameloblastoma: 43, dentigerous cyst: 10) were examined for immunohistochemistry.

RNA isolation

Total RNA was isolated from the frozen dentigerous cyst and ameloblastoma samples. The easy-BLUE^{TM} Total RNA Extraction Kit (iNtRON, Seongnam, South Korea) was used according to the manufacturer's instructions. Total RNA was quantified by spectrophotometer and its integrity was assessed by running on a denaturing 1.0% agarose gel.

Microarray

Profiling of gene expression was analyzed with a GenePlorer^{TM} Human-34K (Digital genomics, Seoul, Korea) consisting of 34 580 genes. About 20 μg of human total RNA was reverse transcribed into cDNA according to the company's protocol. The cDNA

reaction was cleaned up with Microcon YM-30 (Millipore, Billerica, MA, USA) and 2.0 μl of the appropriate NHS-ester Cy dye was added. The coupling reaction was cleaned up with QIAquick PCR purification kit (QIAGEN, Hilden, Germany).

The slides were incubated in pre-hybridization solution and dried by centrifugation. The labeled samples were dried in a hybridization buffer, hybridized, and then incubated in 42°C for more than 16 h. The slides were then washed five times and dried by centrifugation. Hybridization images were scanned by Scanarray Lite (Packard BioChip Technologies, Boston, MA, USA).

Semiquantitative RT–PCR

We validated differential expression of 10 selected overexpressed genes (*VAV3*, *EGFR*, *TOM1L1*, *FUBP1*, *CDK2*, *TNKS*, *PTHRP*, *SMARCA2*, *KLK5*, and *CLU*) and three selected underexpressed genes (*MCC*, *RB1*, and *CDKN1A*) by reverse transcription–polymerase chain reaction (RT–PCR). These genes were chosen because they seemed most pertinent in the development and progression of ameloblastoma. cDNA was synthesized from 1 μg of each of the dentigerous cyst's and ameloblastoma's total RNA, using the SuperScript™ First-strand Synthesis System for RT–PCR (Invitrogen™ Life Technologies, Carlsbad, CA, USA) with an oligo-(dT) primer, according to the manufacturer's directions. The sequence of the primer and expected product sizes for the 13 genes are listed in Table 1. PCR was performed in a total volume of 50 μl, containing 2.5 U of ExTaq DNA polymerase (TaKaRa Biomedicals, Otsu, Japan), 1 μg of cDNA, and 10 pmol of primer. It ran for 30 cycles of denaturation, annealing, and extension each at 95°C for 30 s, 60°C for 30 s, and 72°C for 30 s, respectively. PCR products were separated on a 1% agarose gel and the sizes were determined with a 100 bp DNA ladder. For interpretation of electrophoresis, TINA (Raytest, Wilmington, NC, USA) software was utilized as a densitometer.

Table 1 Sequences of oligonucleotide primers for 10 overexpressed and three underexpressed genes and reverse transcription–polymerase chain reaction (RT–PCR) product sizes

Genes	*Forward (F) and reverse (R) primer sequences*	*Size (bp)*
Overexpressed genes		
FUBP1	F: CAAGCCAAGGAAATGGTGTT	374
	R: ATGTTCCAGTTGCCTTGACC	
VAV3	F: GACCTCAGGGAGATGGTGAA	392
	R: GCAGACTTTGCAGGATGTGA	
TNKS	F: TCTGACCCCTCCATCATCTC	227
	R: AAGTGTAAGGGCGTGGAATG	
PTH1H	F: GGGGAAGTCCATCCAAGATT	306
	R: TCTAACCAGGCAGAGCGAGT	
SMARCA2	F: CCTAGGCGACCTGGAGAAG	211
	R: TTTTGCCTCGGACTCTGACT	
EGFR	F: GGTGCAGGAGAGGAGAACTG	270
	R: GGTGGCACCAAAGCTGTATT	
CDK2	F: GCCCTAATCTCACCCTCTCC	211
	R: AAGGGTGGTGGAGGCTAACT	
TOM1L1	F: TAAAACAGGTCGGGAGATGC	208
	R: GGCAGAAGGCTCACTGGTAG	
KLK5	F: GTCACCAGTTTATGAATCTGGGC	328
	R: GGCGCAGAACATGGTGTCATC	
CLUSTERIN	F: GAGCTCGCCCTTCTACTTCT	619
	R: GTGTTGAGCATCTTCCACTG	
Underexpressed genes		
MCC	F: CACATGGGTGCATTTGTAGC	266
	R: ACTGCCTAGCCCTGTAAGCA	
RB1	F: CACGAATGCAAAAGCAGAAA	375
	R: ACTCCCACTCTAGGGCCATT	
CDKN1A	F: ATGAAATTCACCCCCTTTCC	174
	R: CCCTAGGCTGTGCTCACTTC	

Immunohistochemistry

Immunohistochemical staining was performed using the streptavidin-biotin-peroxidase complex method. About 4 μm thick sections were cut from each paraffin block, de-paraffinized, and incubated for 15 min in methanol solution, containing 3% H_2O_2 to block endogenous peroxidase activity. The slides were then placed in a 0.01 M citrate buffer (pH 6). After washing with phosphate-buffered saline (PBS), sections were incubated in 10% normal rabbit serum for 30 min to reduce non-specific antibody binding. The primary antibody used was goat antihuman polyclonal clusterin antibody (Abcam, Cambridge, UK), at a dilution of 1:500. Each section was incubated for 1 h at room temperature. After washing with PBS, sections were incubated with biotinylated goat antirabbit immunoglobulin G (IgG) for 30 min. They were then washed three times with PBS, treated with streptavidin-peroxidase reagent for 30 min, and re-washed with PBS three times. The reactions were visualized with diaminobenzidine (Dako, Glostrup, Denmark) as a chromogen, and sections were counterstained with Mayer's hematoxylin. Normal rabbit IgG was substituted for each primary antibody as a negative control. Cytoplasmic staining was used to determine positivity. Staining was evaluated as follows: negative if immunoreactivity was observed in fewer than 10% of tumor cells, and positive if observed in more than 10%. Endothelial cells were used as an internal positive control.

Results

Microarray analysis

Overexpression and underexpression were determined using Global *M*-values [$\log_2$ (R/G); R = Cy5 signal − background, G = Cy3 signal − background], acquired after global normalization. Genes whose *M*-values were more than 2 or less than −2 in two independent hybridizations were considered differentially expressed. Of these, 73 genes were overexpressed and 49 were underexpressed. Overexpressed genes were categorized as being involved in the cell cycle and cell growth, transcription and translation, extracellular matrix, adhesion, and invasion, tumor-related proteins, structural proteins, metabolism, cell signaling and signal transduction, and others (Table 2). Underexpressed genes were categorized as being involved in the extracellular matrix, adhesion, and invasion, cytokines, inflammation, and immune response, structural proteins, metabolism, and others (Table 3).

Table 2 Overexpressed genes are more than fourfold in ameloblastoma compared with dentigerous cyst, by means of microarray

Description	*UniGene accession ID*	*Chromosomal localization*
Cell cycle, growth		
Tankyrase trf1-interacting ankyrin-related ADP-ribose polymerase; *TNKS*	NM_003747.1	8p23.1
Cyclin-dependent kinase 2, isoform 2; *CDK2*	NM_052827	12q13
cdc-like kinase 1; clk1	NM_004071	2q33
Protein phosphatase 2 (formerly 2a), regulatory subunit a (pr 65), α-isoform; ppp2r1a	NM_014225	19q13.41
Dual-specificity tyrosine-y-phosphorylation regulated kinase 3; 3 dyrk3	NM_003582	1q32
Ribosomal proteins 4 × isoform; rps4x	NM_001007	Xq13.1
Zinc finger protein 185 (lim domain); znf185	NM_007150	Xq28
Rho guanine nucleotide exchange factor 5; arhgef5	NM_005435	7q33-q35
Dual specificity phosphatase isoform b; dusp6	NM_022652	12q22-q23
Glypican4; gpc4	NM_001448	Xq26.1
Transcription, translation		
u5snrnp-specific protein; prpf8	NM_006445	17p13.3
pro2047 protein; ppp1r8	NM_014110	1p35
Zinc finger protein 278 short isoform; znf278	NM_032051.1	22q12.2
btg family, member 2; btg2	NM_006763	1q32
Eukaryotic translation elongation factor 2; eef2	NM_001961	19pter-q12
Paired-like homeodomain transcription factor 2; pitx2	NM_000325	4q25-q27
Eukaryotic translation initiation factor 3, subunit 8 (110 kDa); eif3s8	NM_003752	16p11.2
swi/snf-related, matrix-associated, actin-dependent regulator of chromatin, subfamily a, member 2; *SMARCA2*	NM_003070	9p22.3
Tripartite motif protein trim 29, isoform-α; trim29	NM_012101	11q22-q23
General transcription factor ii, i, isoform 3; gtf2i	NM_033001	7q11.23
Nuclear factor, interleukin-3 regulated; nfil3	NM_005384	9q22
Max-interacting protein 1; mxi1	NM_005962	10q24-q25
Far upstream element-binding protein; *FUBP1*	NM_003902	1p31.1
ECM, adhesion, invasion		
Neogenin homolog 1 (chicken); neo1	NM_002499	15q22.3-q23
α-5 type iv collagen isoform 2; col4a5	NM_033380	Xq22
kallikrein 3 (prostate-specific antigen); klk3	NM_001648	19q13.41
kallikrein 4 (prostase, enamel matrix, prostate); klk4	NM_004917	19q13.41
kallikrein 5; *KLK5*	NM_012427	19q13.3-q13.4
Tumor-related protein		
Suppression of tumorigenicity 5; st5	NM_005418	11p15
v-crkaviansarcoma virus ct10 oncogene homolog isoform a; crk	NM_016823	17p13.3
Epidermal growth factor receptor [erythroblastic leukemia viral (v-erb-b) oncogene homolog, avian]; *EGFR*	NM_005228	7p12
vav3 oncogene; *VAV3*	NM_006113	1p13.3
Tumor-related protein; c1orf10	NM_016190	1q21
Structure protein		
Microtubule-associated protein 2, isoform 2; map2	NM_031845	2q34-q35
Actinin, α-4; actn4	NM_004924	19q13
Troponini, cardiac; tnni3	NM_000363	19q13.4
Erythrocyte membrane protein band 4.9 (dematin); epb49	NM_001978	8p21.1
Tubulin, γ-1; tubg1	NM_001070	17q21
Profilin 2 isoform b; pfn2	NM_002628	3q25.1-q25.2
Metabolism		
Sterol-c4-methyloxidase-like; sc4mol	NM_006745	4q32-q34
Branched chain keto acid dehydrogenase e1, α-polypeptide (maple syrup urine disease); bckdha	NM_000709	19q13.1-q13.2
Methionine adenosyltransferase ii, α; mat2a	NM_005911	2p11.2
NADP-dependent leukotriene b4 12-hydroxydehydrogenase; ltb4dh	XM_088569	9q32
Cell signaling, signal transduction		
Shb adaptor protein (a src homology 2 protein); shb	NM_003028	9p12-p11
Epha4	NM_004438	2q36.1
Rho guanine nucleotide exchange factor 3; arhgef3	NM_019555	3p21-p13
Pdz domain protein (regulated *Drosophila* inad-like); inadl	NM_005799	1p32.1
Target of myb1-like 1 (chicken); *TOM1L1*	NM_005486	17q23.2
Protein kinase C substrate 80k-h; prkcsh	NM_002743	19p13.2
Iq motif-containing GTPase-activating protein 2; iqgap2	NM_006633	5q13.3-q14.1
Epha7	NM_004440	6q16.1
Syntaxin16; stx16	NM_003763	20q13.32
RNA-binding motif protein 14; rbm14	NM_006328	11q13.1
Carboxypeptidase E precursor; cpe	NM_001873	4q32.3
Parathyroid hormone-like hormone; pthlh	NM_002820	12p12.1-p11.2
Mitogen-activated protein kinase 10; mapk10	NM_002753	4q22.1-q23

Table 2 Continued

Description	*UniGene accession ID*	*Chromosomal localization*
Others		
Pleckstrin homology-like domain, family a, member 1; phlda1	NM_007350	12q15
Protease inhibitor 12 (neuroserpin); serpini1	NM_005025	3q26.2
Arg99 protein	NM_031920.1	12p11.23
Gene33/mig-6; mig-6	NM_018948	1p36.12-36.33
Hypothetical protein; flj20323	NM_019005	7p22-p21
Impinosine monophosphate dehydrogenase 2; impdh2	NM_000884	3p21.2
Chromosome 1 open-reading frame 9; c1orf9	NM_014283	1q24
Mitochondrial ribosomal protein l4; mrpl4	NM_015956	10q24.31
Damage-specific DNA-binding protein 1; ddb1	NM_001923	11q12-q13
Ribosomal proteins 3; rps3	NM_001005	11q13.3-q13.5
Ornithine decarboxylase 1; odc1	NM_002539	2p25
RNA-binding motif protein, X-chromosome; rbmx	NM_002139	Xq26
Mitochondrial intermediate peptidase; mipep	NM_005932	13q12
RNA-binding protein (autoantigenic) long isoform; raly	NM_016732	20q11.21-q11.23
G protein-coupled receptor 48; gpr48	NM_018490	11p14-p13
Progesterone receptor-associated p48 protein; st13	NM_003932	22q13.2
Clusterin (complement lysis inhibitor, sp-40,40, sulfated glycoprotein 2, testosterone-repressed prostate message 2, apolipoprotein j); clu	NM_001831	8p21-p12

Semiquantitative RT–PCR

The 10 overexpressed genes and three underexpressed genes, whose functions seemed most pertinent in the development and progression of ameloblastoma, were selected after a literature review of current research trends. Quantitative verification of the microarray results was performed through RT–PCR and densitometric analysis. The results were normalized by the amount of PCR products that were amplified for GAPDH expression. Data were presented as mean ± SEM with values derived from at least three separate, independent experiments. The results of the semiquantitative RT–PCR analysis are illustrated in Fig. 1. All of the results corroborated our microarray data.

Immunohistochemistry

Clusterin, verified to be overexpressed in ameloblastoma by RT–PCR, was selected for immunohistochemistry staining in order to validate its expression at the protein level (Fig. 2). Ameloblastoma presented positive staining in 76.7% of samples (10 of 43), while the dentigerous cyst presented 50% (five of 10). Ameloblastoma cases tended to show higher level of clusterin expression, but not at a statistical level ($P = 0.124$).

Discussion

In order to investigate the factors involved in the transformation from dentigerous cyst to ameloblastoma on a genetic level, we performed a microarray experiment to examine the differences in the levels of gene expression of the two. Microarray analysis is a powerful tool for the global characterization of gene expression. Our study used oligonucleotide microarray instead of the cDNA system. The oligonucleotide system is considered to be more exact because oligonucleotide probes are shorter than cDNA probes. As hybridization conditions are based on the length of nucleic acid fragments and the compositions of G + C and A + T (or A + U), hybridization efficiency can vary widely when long cDNA sequences are used as a probe (8).

Many underexpressed genes were cytokines or involved in inflammation and immune responses. Some underexpressed genes that may play a role in the suppression of tumorigenesis are *MCC*, *RB1*, and *CDKN1A*. *MCC* (mutated in colorectal cancer) is a tumor-suppressor gene (9). *CDKN1A* and *RB1* work together in the cell cycle and are affected by p53 (10). As an inhibitor of cyclin-dependent kinases, *CDKN1A* is known to prevent the phosphorylation of retinoblastoma (RB) family proteins and hence leads to transcriptional repression (11). In Carinci et al.'s study comparing odontogenic tumors to normal gum mucosa, genes encoding for DNA repair enzymes, protein synthesis, and basement membrane were underexpressed (7). The functions of underexpressed genes in our study were slightly different, perhaps owing to differences in the control specimens. In Heikinheimo et al.'s (6) study comparing ameloblastoma to tooth germs, TGFB1, SHH, and CDH11 were underexpressed. These genes, judging from their *M*-values, were not differentially expressed in our study.

Most overexpressed genes in our study were involved in tumorigenic processes, such as the cell cycle and growth, transcription, and translation. In Carinci et al's study, genes encoding for similar functions such as intercellular adhesion and extracellular matrix, signaling of cell growth and differentiation, and oxidative metabolism were overexpressed. In Heikinheimo et al.'s (6) study, FOS (a proto-oncogene), TNFR1A (involved in cell proliferation and differentiation), and COL8A1 (involved in cell adhesion) were overexpressed. These genes also play similar functions to the ones in our study. Overexpressed genes from our study that may play important roles in the tumorigenesis of ameloblastoma, based on recent research, are *VAV3*, *EGFR*, *TOM1L1*, *FUBP1*, *CDK2*, *TNKS*, *PTHRP*, *SMARCA2*, *KLK5*, and *CLU*.

Table 3 Genes underexpressed are more than fourfold in ameloblastoma compared with dentigerous cyst, by means of microarray

Description	*UniGene accession ID*	*Chromosomal localization*
ECM, cell adhesion, invasion		
Collagen, typexi, α-1; col11a1	NM_001854	1p21
Integrin-β chain, β-2 precursor; itgb2	NM_000211	21q22.3
Matrix metalloproteinase 7; mmp7	NM_002423	11q21-q22
s100 calcium-binding protein a4; s100a4	NM_019554	1q21
Osteomodulin; omd	NM_005014	9q22.32
Disintegrin protease; adamdec1	NM_014479	8p21.2
Dermatopontin precursor; dpt	NM_001937	1q12-q23
Hyaluronan-binding protein 2; habp2	NM_004132	10q26.11
Secreted phosphoprotein 1 (osteopontin, bone sialoprotein i, early T-lymphocyte activation 1); spp1	NM_000582	4q21-q25
Centrosomalp4.1-associated protein; cpap	NM_018451	13q12.13
Cytokine, inflammation, immune response		
Histaminen-methyltransferase; hnmt	NM_006895	2q22.1
Microsomal glutathiones-transferase 2; mgst2	NM_002413	4q28.3
Serine carboxypeptidase vitellogenic-like; cpvl	NM_031311	7p15-p14
Adipsin/complement factor d precursor; df	NM_001928	19p13.3
Cathepsins; ctss	NM_004079	1q21
Myeloid cell nuclear differentiation antigen; mnda	NM_002432	1q22
cd14 antigen precursor; cd14	NM_000591	5q22-q32
md-2 protein; md-2	NM_015364	8q13.3
Interferon, γ-inducible protein 30; ifi30	NM_006332	19p13.1
Killer cell lectin-like receptor subfamily b, member 1; klrb1	NM_002258	12p13
Structural protein		
Vimentin; vim	NM_003380	10p13
p25	AF334588	5p15.3
Metabolism		
Mannosyl (α-1,3)-glycoprotein β-1,4-*n*-acetylglucosaminyl transferase, isoenzyme a; mgat4a	NM_012214	2q12
Fructose-1,6-bisphosphatase 1; fbp1	NM_000507	9q22.3
Kynureninase(l-kynureninehydrolase); kynu	NM_003937	2q22.3
Guanosine monophosphate reductase; gmpr	NM_006877	6p23
NAD(P)H menadione oxidoreductase 1, dioxin-inducible; nqo1	NM_000903	16q22.1
Aldehyde dehydrogenase 1, soluble; aldh1	NM_000689	9q21.13
Low-density lipoprotein-related protein 2; lrp2	NM_004525	2q24-q31
Cytochrome p450, subfamily i (dioxin-inducible), polypeptide 1; cyp1b1	NM_000104	2p21
Others		
High-affinity immunoglobulin ϵ-receptor β-subunit; ms4a7	NM_021201	11q12
Mannose receptor, c type 1; mrc1	NM_002438	10p13
Cholinergic receptor, nicotinic, γ-polypeptide; chrng	NM_005199	2q33-q34
NAD(P)H dehydrogenase, quinone 2; nqo2	NM_000904	6pter-q12
SQRDL		15q15
Mutated in colorectal cancers; *MCC*	NM_002387	5q21-q22
Ubiquitin carboxyl-terminal esterase l1 (ubiquitin thiolesterase); uchl1	NM_004181	4p14
Hypothetical protein impact; impact	NM_018439	18q11.2-q12.1
Lysozyme precursor; lyz	NM_000239	12q14.3
Cyclin-dependent kinase inhibitor 1A (p21, Cip1); *CDKN1A*	NM_078467	6p21.2
Sam domain, sh3 domain and nuclear localization signals 1; samsn1	NM_022136	21q11
Solute carrier family 11 (proton-coupled divalent metal ion transporters), member 3; slc11a3	NM_014585	2q32
ATP synthase, H^+-transporting, mitochondrial f0 complex, subunit c (subunit 9) isoform 3; atp5g3	NM_001689	2q31.2
Polio virus receptor-related herpes virus entry mediator b; pvrl2	XM_044320	19q13.2-q13.4
Kallikrein-like protein klk9 alternatively spliced; klk-l3; spliced	AF135026	19q13.41
Retinoblastoma 1; *RB1*	NM_000321	13q14.2
TATA box-binding protein (tbp)-associated factor, RNA polymerase ii, k, 18 kDa; taf2k	NM_005645	1p13.1
bcl2-associated athanogene 2; bag2	NM_004282	6p12.3-p11.2
Colony-stimulating factor 1 receptor, formerly mcdonough feline sarcoma viral (v-fms) oncogene homolog; csf1r	NM_005211	5q33-q35

VAV3 is a guanine nucleotide exchange factor and seems to be significant in regulating the downstream pathway in Rho signaling (12). A recent study showed that *VAV3* was upregulated during mitosis (13), a feature not demonstrated by other VAV family members. Therefore, *VAV3* might be a marker indicating the extensive proliferative activity of ameloblastoma, compared with dentigerous cyst.

Binding of *EGFR* to its ligands activates two major signaling pathways, the Ras-Raf mitogen-activated protein kinase pathway (14) and the phosphatidyl inositol-3′ kinase and Akt pathway (15–17). These

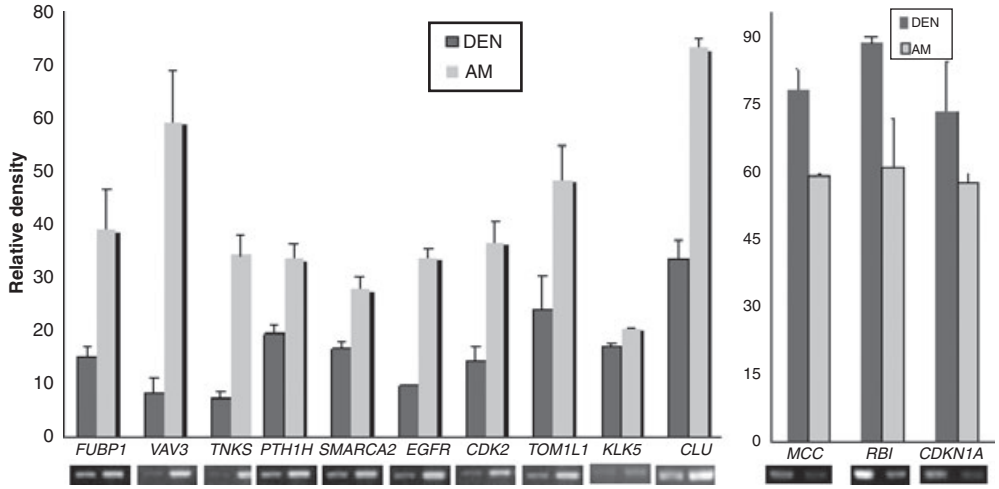

Figure 1 Semiquantitative reverse transcription–polymerase chain reaction (RT–PCR) analysis and expression patterns of 10 upregulated and three downregulated genes (den, dentigerous cyst; am, ameloblastoma).

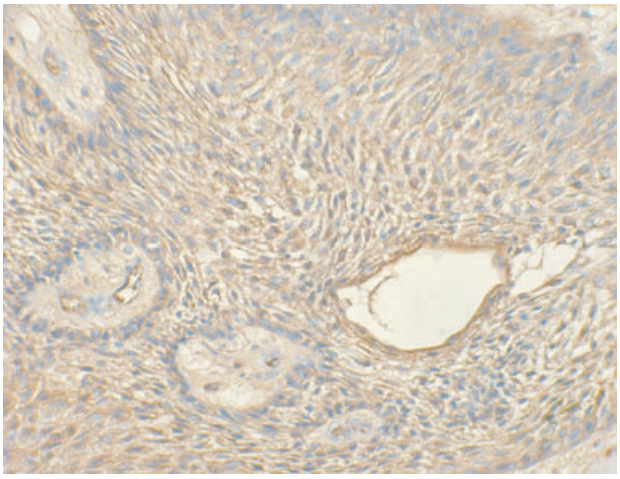

Figure 2 Representative immunohistochemical reactivity for *CLU* in ameloblastomas. Positive staining: cytoplasmic and diffuse background reactivity (×200).

pathways are involved in many biologic functions that contribute to tumorigenesis (18). Vered et al. reported that overexpression of *EGFR* in ameloblastoma (19).

TOM1L1 is a FYN substrate that can stimulate kinase autophosphorylation. FYN, a member of Src family kinases (SFKs), is implicated in the control of cell growth (20). *FUBP1* is an essential transcription factor for *c-myc* proto-oncogene expression. The *c-myc* gene is involved in cell growth, proliferation, differentiation, apoptosis, and the induction of telomerase activity, therefore contributing to tumorigenesis (21–23). Kumamoto et al. have already demonstrated the expression of *c-myc* in ameloblastoma using immunohistochemistry (24).

CDK2 is an indispensable molecular player in the cell cycle and is activated by cyclin E or cyclin A. It is involved in the transition from the G1 to S phase (25, 26). Many studies showed that *CDK2* dominant-negative mutants block cell progression, suggesting *CDK2*/cyclin E deregulation to be implicated in tumorigenesis (26).

Tankyrase 1, a poly(ADP-ribose) polymerase (PARP), promotes telomere elongation (27), therefore allowing tumor cells to grow continuously (28). Tankyrase 1 increases access of telomerase to telomeres by releasing TRF1 from the telomeres (29). TRF1 is known to induce bending of telomeric DNA into t-loops, limiting access of telomerase to telomeres (30).

PTHRP has been proven to be expressed in ameloblastoma through immunohistochemistry, by Abdelsayed et al. (31). *PTHRP* expression by ameloblastoma target receptors in the surrounding bone, subsequently cause resorption and facilitate tumor growth. An interesting finding in that study was that the non-ameloblastic lining epithelium of the dentigerous cyst samples did not express *PTHRP*. This suggests that *PTHRP*-mediated bone resorption may play a significant role in the growth of ameloblastoma, but not in dentigerous cysts (31).

KLK5 has been isolated from the stratum corneum of the epidermis and is proposed to function in the degradation of intercellular structures, such as desmosomes (32–34). Also, Borgono et al. suggested that *KLK5* is able to cleave components of the extracellular matrix *in vitro*, therefore functioning in tissue remodeling in a similar way to matrix metalloproteinases (35).

CLU is a widely expressed glycoprotein implicated in diverse physiologic processes and several human cancers (36). This gene has two different isoforms (37, 38). The nuclear form (50 kDa), which is believed to play a proapoptotic function (39) is unglycosylated and localizes to the nucleus, while the secreted form (40 kDa) is glycosylated and can be found in the cytoplasm (36). The secreted form has been attributed with cytoprotective and antiapoptotic functions against various stress agents (40, 41). The role of secreted clusterin in promoting tumor progression is supported by the fact that this secreted form has been identified in the cytoplasm, but not the nucleus, of highly infiltrating tumors and metastatic nodes (36, 42). Our immuno-

histochemical results also demonstrated clusterin only in the cytoplasm, not the nucleus, of ameloblastoma cells. The diffuse background staining that was observed may be related to the implicated role of Clusterin in stimulating cell motility and invasive ability (43).

According to Trougakos and Gonos, clusterin's role in tumorigenesis can be summed up into three activities: inhibition of apoptosis, involvement in cell–cell and cell–substratum interactions during anchorage-independent growth, and a cytoprotective role in the plasma membrane by preventing deleterious contact with cytolytic proteins (42). Thus, overexpression of clusterin may contribute to the immortality and aggressive behavior of ameloblastoma cells.

In conclusion, we identified important genes that are related to the development and progression of ameloblastoma through a large-scale gene expression analysis using microarray. Although more research will be necessary to clarify the molecular pathways of these genes in relation to ameloblastoma tumorigenesis, our study will provide a basis for further research that will contribute to the development of early diagnostic and prognostic factors for ameloblastoma.

References

1. Kramer IR, Pindborg JJ, Shear M. The World Health Organization histological typing of odontogenic tumours. Introducing the second edition. *Eur J Cancer B Oral Oncol* 1993; **29B**: 169–71.
2. Neville BW, Damm DD, Allen CM, Bouquot JE. *Oral and maxillofacial pathology*, 2 edn. Philadelphia, USA: W.B. Saunders Company, 2002.
3. Kahn MA. Ameloblastoma in young persons: a clinicopathologic analysis and etiologic investigation. *Oral Surg Oral Med Oral Pathol* 1989; **67**: 706–15.
4. Leider AS, Eversole LR, Barkin ME. Cystic ameloblastoma. A clinicopathologic analysis. *Oral Surg Oral Med Oral Pathol* 1985; **60**: 624–30.
5. Sonesson A. Odontogenic cysts and cystic tumours of the jaws. A roentgen-diagnostic and patho-anatomic study. *Acta Radiol Suppl* 1950; **81**: 1–159.
6. Heikinheimo K, Jee KJ, Niini T, et al. Gene expression profiling of ameloblastoma and human tooth germ by means of a cDNA microarray. *J Dent Res* 2002; **81**: 525–30.
7. Carinci F, Francioso F, Piattelli A, et al. Genetic expression profiling of six odontogenic tumors. *J Dent Res* 2003; **82**: 551–7.
8. Li J, Pankratz M, Johnson JA. Differential gene expression patterns revealed by oligonucleotide versus long cDNA arrays. *Toxicol Sci* 2002; **69**: 383–90.
9. Kinzler KW, Nilbert MC, Vogelstein B, et al. Identification of a gene located at chromosome 5q21 that is mutated in colorectal cancers. *Science* 1991; **251**: 1366–70.
10. el-Deiry WS, Tokino T, Velculescu VE, et al. WAF1, a potential mediator of p53 tumor suppression. *Cell* 1993; **75**: 817–25.
11. Bartek J, Lukas J. Pathways governing G1/S transition and their response to DNA damage. *FEBS Lett* 2001; **490**: 117–22.
12. Katzav S. Vav: Captain Hook for signal transduction? *Crit Rev Oncog* 1995; **6**: 87–97.
13. Fujikawa K, Inoue Y, Sakai M, et al. Vav3 is regulated during the cell cycle and effects cell division. *Proc Natl Acad Sci U S A* 2002; **99**: 4313–8.
14. Alroy I, Yarden Y. The ErbB signaling network in embryogenesis and oncogenesis: signal diversification through combinatorial ligand-receptor interactions. *FEBS Lett* 1997; **410**: 83–6.
15. Burgering BM, Coffer PJ. Protein kinase B (c-Akt) in phosphatidylinositol-3-OH kinase signal transduction. *Nature* 1995; **376**: 599–602.
16. Liu W, Li J, Roth RA. Heregulin regulation of Akt/protein kinase B in breast cancer cells. *Biochem Biophys Res Commun* 1999; **261**: 897–903.
17. Muthuswamy SK, Gilman M, Brugge JS. Controlled dimerization of ErbB receptors provides evidence for differential signaling by homo- and heterodimers. *Mol Cell Biol* 1999; **19**: 6845–57.
18. Chan TO, Rittenhouse SE, Tsichlis PN. AKT/PKB and other D3 phosphoinositide-regulated kinases: kinase activation by phosphoinositide-dependent phosphorylation. *Annu Rev Biochem* 1999; **68**: 965–1014.
19. Vered M, Shohat I, Buchner A. Epidermal growth factor receptor expression in abeloblastoma. *Oral Oncol* 2003; **39**: 138–43.
20. Seykora JT, Mei L, Dotto GP, Stein PL. SRCASM: a novel Src activating and signaling molecule. *J Biol Chem* 2002; **277**: 2812–22.
21. He L, Liu J, Collins I, et al. Loss of FBP function arrests cellular proliferation and extinguishes c-myc expression. *EMBO J* 2000; **19**: 1034–44.
22. Takakura M, Kyo S, Kanaya T, et al. Cloning of human telomerase catalytic subunit (hTERT) gene promoter and identification of proximal core promoter sequences essential for transcriptional activation in immortalized and cancer cells. *Cancer Res* 1999; **59**: 551–7.
23. Wu KJ, Grandori C, Amacker M, et al. Direct activation of TERT transcription by c-MYC. *Nat Genet* 1999; **21**: 220–4.
24. Kumamoto H, Kinouchi Y, Ooya K. Telomerase activity and telomerase reverse transcriptase (TERT) expression in ameloblastomas. *J Oral Pathol Med* 2001; **30**: 231–6.
25. Sherr CJ. The Pezcoller lecture: cancer cell cycles revisited. *Cancer Res* 2000; **60**: 3689–95.
26. van den Heuvel S, Harlow E. Distinct roles for cyclin-dependent kinases in cell cycle control. *Science* 1993; **262**: 2050–4.
27. Bae J, Donigian JR, Hsueh AJ. Tankyrase 1 interacts with Mcl-1 proteins and inhibits their regulation of apoptosis. *J Biol Chem* 2003; **278**: 5195–204.
28. Cook BD, Dynek JN, Chang W, Shostak G, Smith S. Role for the related poly(ADP-ribose) polymerases tankyrase 1 and 2 at human telomeres. *Mol Cell Biol* 2002; **22**: 332–42.
29. Smith S, Giriat I, Schmitt A, de Lange T. Tankyrase, a poly(ADP-ribose) polymerase at human telomeres. *Science* 1998; **282**: 1484–7.
30. Griffith JD, Comeau L, Rosenfield S, et al. Mammalian telomeres end in a large duplex loop. *Cell* 1999; **97**: 503–14.
31. Abdelsayed RA, Vartanian RK, Smith KK, Ibrahim NA. Parathyroid hormone-related protein (PTHrP) expression in ameloblastoma. *Oral Surg Oral Med Oral Pathol Oral Radiol Endod* 2004; **97**: 208–19.
32. Ekholm IE, Brattsand M, Egelrud T. Stratum corneum tryptic enzyme in normal epidermis: a missing link in the desquamation process? *J Invest Dermatol* 2000; **114**: 56–63.

33. Lundstrom A, Egelrud T. Cell shedding from human plantar skin in vitro: evidence that two different types of protein structures are degraded by a chymotrypsin-like enzyme. *Arch Dermatol Res* 1990; **282**: 234–7.
34. Lundstrom A, Egelrud T. Evidence that cell shedding from plantar stratum corneum in vitro involves endogenous proteolysis of the desmosomal protein desmoglein I. *J Invest Dermatol* 1990; **94**: 216–20.
35. Borgono CA, Michael IP, Diamandis EP. Human tissue kallikreins: physiologic roles and applications in cancer. *Mol Cancer Res* 2004; **2**: 257–80.
36. Pucci S, Bonanno E, Pichiorri F, Angeloni C, Spagnoli LG. Modulation of different clusterin isoforms in human colon tumorigenesis. *Oncogene* 2004; **23**: 2298–304.
37. Lakins J, Bennett SA, Chen JH, et al. Clusterin biogenesis is altered during apoptosis in the regressing rat ventral prostate. *J Biol Chem* 1998; **273**: 27887–95.
38. Reddy KB, Jin G, Karode MC, Harmony JA, Howe PH. Transforming growth factor beta (TGF beta)-induced nuclear localization of apolipoprotein J/clusterin in epithelial cells. *Biochemistry* 1996; **35**: 6157–63.
39. Scaltriti M, Santamaria A, Paciucci R, Bettuzzi S. Intracellular clusterin induces G2-M phase arrest and cell death in PC-3 prostate cancer cells1. *Cancer Res* 2004; **64**: 6174–82.
40. Wu AJ, Park II, Zhaung L, Lee C. Response to a lethal dose of heat shock by a transient up-regulation of clusterin expression followed by down-regulation and apoptosis in prostate and bladder cancer cells. *Prostate* 2002; **53**: 277–85.
41. Sensibar JA, Sutkowski DM, Raffo A, et al. Prevention of cell death induced by tumor necrosis factor alpha in LNCaP cells by overexpression of sulfated glycoprotein-2 (clusterin). *Cancer Res* 1995; **55**: 2431–7.
42. Trougakos IP, Gonos ES. Clusterin/apolipoprotein J in human aging and cancer. *Int J Biochem Cell Biol* 2002; **34**: 1430–48.
43. Miyake H, Gleave ME, Arakawa S, Kamidono S, Hara I. Introducing the clusterin gene into human renal cell carcinoma cells enhances their metastatic potential. *J Urol* 2002; **167**: 2203–8.